2014-08-08

# Functional Roles of Syngap1 in Early Embryonic Development of Zebrafish

Bing Zou
*University of Miami*, zoubing1989@gmail.com

UNIVERSITY OF MIAMI

# FUNCTIONAL ROLES OF *SYNGAP1* IN EARLY EMBRYONIC DEVELOPMENT OF ZEBRAFISH

By

Bing Zou

A THESIS

Submitted to the Faculty
of the University of Miami
in partial fulfillment of the requirements for
the degree of Master of Science

Coral Gables, Florida

August 2014

UNIVERSITY OF MIAMI

A thesis submitted in partial fulfillment of
the requirements for the degree of
Master of Science

# FUNCTIONAL ROLES OF *SYNGAP1* IN EARLY EMBRYONIC DEVELOPMENT OF ZEBRAFISH

Bing Zou

Approved:

| | |
|---|---|
| _____<br>Julia Dallman, Ph.D.<br>Assistant Professor of Biology | _____<br>Athula Wikramanayake, Ph.D.<br>Professor of Biology |
| _____<br>Zhongmin Lu, Ph.D.<br>Associate Professor of Biology | _____<br>M. Brian Blake, Ph.D.<br>Dean of the Graduate School |

_____
Katherina Walz, Ph.D.
Assistant Professor of John P. Hussman
Institute for Human Genomics

ZOU, BING (M.S., Biology)

Functional Roles of *Syngap1* In Early Embryonic Development of Zebrafish (August 2014)

Abstract of a thesis at the University of Miami.

Thesis supervised by Professor Julia Dallman.
No. of pages in text. (51)

*De novo* mutations of *SYNGAP1* (Synaptic GTPase Activating Protein) have been found in human patients with intellectual disability, epilepsy and autism. Consistent with an important role for *SYNGAP1* in nervous system development, mice heterozygous for *SYNGAP1* loss-of-function mutations exhibit disrupted behavior and cognition. Studies in mice have focused on the role of *SYNGAP1* at excitatory post-synapses even though *SYNGAP1* is expressed prior to synaptogenesis. To study the potential roles of *SYNGAP1* during early developmental stages, we carried out a *syngap1* morpholino study in zebrafish and found that knockdown of *syngap1* causes reduced brain size, increased cell death in the brain and spinal cord before synaptogenesis and disrupted behaviors. We also found decreased GABAergic precursors in *syngap1b* morphants and increased apoptosis in the GABAergic progenitor area. These findings bridge the gap between embryonic mutations and later phenotypes, supporting the emerging view of prenatal origin in etiology of neurodevelopmental disorders associated with autism spectrum disorders.

## TABLE OF CONTENTS

Page

**List of Figures**

Page

**List of Tables**

Page

## Introduction

Neurodevelopmental disorders, such as autism spectrum disorders (ASD), intellectual disability (ID) and epilepsy, are disabilities primarily associated with brain dysfunction (Axelrad et al., 2013). An increasing number of individuals affected by neurodevelopmental disorders have been reported recently. For example, the prevalence of ID is approximately 1% of worldwide population (Kupfer et al., 2013) and every social class and culture is affected (Leonard and Wen 2002). ASD is estimated to affect 1-2.6% of children world-wide (Kogan et al., 2009; Kim et al., 2011). And about 50 million people worldwide are affected by epilepsy (WHO epilepsy fact sheet, 2012). As a result of the increasing prevalence, understanding the mechanisms behind these neurodevelopmental disorders has become a research priority.

Neurodevelopmental disorders have been linked to mutations in specific genes and chromosomal loci (Mitchell 2011). Mounting evidence has implicated mutations in genes that start functioning in the early embryo (Hallmayer et al., 2011; Goldman et al., 2009; Pinto et al., 2010; Sebat et al., 2007; Ropers 2008) suggesting the possibility that symptoms used to diagnose young children with neurodevelopmental disorders have mechanistic underpinnings that start in the embryo. Consistent with this idea, postmortem studies of neocortex tissues from autistic and neurotypical children found abnormal focal patches of cortical laminar cytoarchitecture and disorganization of neurons in cortices of the majority of autistic children. Because cortical layering is established at embryonic stages, these results indicate a prenatal origin of brain structural deficits associated with

autism (Stoner et al., 2014). In accordance with this idea, transcriptome analysis of the human pre-natal brain revealed patterned expression of many brain-disorder-related genes, including *SYNGAP1*, *SHANK3* and *RELN*, indicating that dysfunctions of these genes in early embryonic stages may confer a predisposition to neurodevelopmental disorders such as ASD, ID and epilepsy (Miller et al., 2014). Gene co-expression network analysis using human post-mortem brain tissues demonstrated consistent differences in transcriptomes from autistic and neurotypical brains. Moreover, expressions in frontal and temporal cortex of autism brain were more similar than neurotypical brains suggesting defects of cortical patterning in autism brain (Voineagu et al., 2011). This evidence indicates that prenatal genetic mutations which affect embryonic brain development play an important role in etiology of neurodevelopmental disorders.

### *SYNGAP1 de novo* mutations are linked to non-syndromic intellectual disability (NS-ID), epilepsy and autism

*De novo* mutations (found in the offspring but not in the parents) in the *SYNGAP1* gene have been found in human patients with non-syndromic intellectual disability (NS-ID), ASD and epilepsy (Hamdan et al., 2011; Hamdan et al., 2009). NS-ID has been defined by the presence of intellectual disability as the sole clinical feature without presence of morphological or metabolic deficits (Kaufman et al., 2010). Therefore, these mutations result from a mutation in sperm or egg, or in the fertilized egg itself (Pagon et al., 2013). Since the *de novo* mutations found in patients are new to the genome, and none of them were found in control individuals, therefore they are likely to be important to the

etiology of that disorder. Three *de novo* truncating mutations in *SYNGAP1* (K138X, R579X, and L813RfsX22) were identified in 3 of 94 patients with NS-ID, indicating disruption of *SYNGAP1* is a common cause of autosomal dominant NS-ID (Hamdan et al., 2009). More recently, *de novo* deletions (c.2677delC/p.Q893RfsX184 and c.321_324delGAAG/p. K108VfsX25) that truncate *SYNGAP1* by disrupting the reading frame were identified in two patients with NS-ID and mild epilepsy, and a *de novo* splicing mutation (c.2294 + 1G>A) which causes pre-mature stop codon was found in a patient with NS-ID and autism (Hamdan et al., 2011). Significantly none of these splicing or truncating mutations have been found in control individuals (healthy individuals without these disorders). This enrichment of *de novo* mutations in individuals with NS-ID provides evidence that *de novo SYNGAP1* mutations are likely to be pathogenic, and suggests that the *SYNGAP1* gene plays an important role in normal brain functions (Hamdan et al., 2011).

SYNGAP1 is an abundant 140-kDa protein found at high concentrations in the brain excitatory postsynaptic density fractions consistent with a role for this protein in nervous system function. In humans, there is only one copy of the *SYNGAP1* gene on chromosome 6, but there are two copies of *syngap1* in zebrafish because of genome duplication. One of these copies is on chromosome 19 (*syngap1a*) and the other is on chromosome 16 (*syngap1b*) (**Fig. 1**).

There are several conserved domains in the SYNGAP1 protein that are suggestive of its functional role in neurons (**Fig. 1**). These domains include a

RasGAP (Ras GTPase-activating proteins) domain, which enhances the endogenous GTPase activity of Ras, via its C-terminal GAP domain; PH (pleckstrin homology) domain, which can bind to phospholipids and might act as a membrane recruitment module; C2 domain, which has been studied as a $Ca^{2+}$ dependent phospholipid-binding molecule (Nalefski et al., 1996) in various signaling pathways and has been found to be essential for stimulation of Rap GTPases (Pena et al., 2008); C-terminal motif required for binding to PDZ (Chen et al., 1998) domains of postsynaptic proteins such as PSD-95 and SAP102, which facilitates the interaction of *SYNGAP1* with NMDA receptors (Chen et al., 1998). The *de novo* mutations found in *SYNGAP1* of human patients all cause truncation of SYNGAP1 protein, resulting in loss of one functional copy of *SYNGAP1*, suggesting *SYNGAP1* heterozygotes are haploinsufficient and may cause pathology.

Expression patterns of *Syngap1* have been studied in multiple organisms but most thoroughly in mice and rats (Chen et al., 1998; Kim 1998; Porter et al., 2005; Petralia et al., 2005). In mouse, *Syngap1* shows a much higher expression in the brain than other tissues as shown by a multiple-tissue northern bolt for *Syngap1* (Chen et al., 1998). Immunoblots of rat tissues with SYNGAP1 antibody demonstrated a high level of *Syngap1* expression in brain, with enrichment in the cortex, hippocampus and olfactory bulb (Kim 1998). Immunohistochemistry using antibodies against SYNGAP1, the NR1 subunit of NMDA receptor (to label excitatory synapses) and anti-glutamic acid decarboxylase (to label inhibitory synapses) showed that SYNGAP1 co-localizes with NMDA receptors and was

present at all excitatory synapses (Kim 1998). In adult mouse brain, the expression pattern of *SYNGAP1* was shown to be further restricted to the anterior of adult forebrain (Porter et al., 2005). Expression of *Syngap1* shows both distinct and overlapping patterns compared to PSD-95 from embryonic stages to adult: *Syngap1* expression peaked during synaptogenesis while PSD-95 expressed throughout the brain from early embryonic stages. Furthermore, *Syngap1* showed a more spatially restricted pattern to forebrain while PSD-95, was also found in mid- and hindbrain (Porter et al., 2005). Immunogold labeling of SYNGAP1 to determine its ontogeny at glutamatergic synapses, indicated that *Syngap1* is moderately prevalent at all ages, and increases significantly from P10 to P35 (Petralia et al., 2005). Taken together the *de novo* mutation studies of *SYNGAP1* in human and expression studies of *Syngap1* in mouse/rat, we can speculate on the potential embryonic roles of *SYNGAP1* in brain morphogenesis and patterning, disruption of which is causally associated with various neurodevelopmental disorders.

**Disrupted E/I balance - a potential mechanism of neurodevelopmental disorders linked to *SYNGAP1* haploinsufficiency**

Establishing and maintaining an appropriate ratio of excitatory versus inhibitory neurotransmission is critical for normal brain functions and brain's plasticity, or brain's capacity for change (Bavelier et al., 2010). Early in development, E/I balance is skewed towards excitation (Wehr et al., 2003; Mittmann et al., 2005; Wilent et al., 2005; Higley et al., 2006). As development progresses, inhibitory signaling increases to match excitatory signaling, sculpting

critical periods which are time windows when brain is readily shaped by a combination of gene expression and environmental experience (Bavelier et al., 2010).

Disruption of E/I balance is thought to underlie several neurodevelopmental disorders (Yizhar et al., 2011; Gatto et al., 2010). For instance, autism has been suggested to result from an increased ratio of excitation/inhibition in nervous system (Rubenstein et al., 2003). Epilepsy, characterized by repeated seizures over time, has been indicated to disrupt E/I balance associated with GABA (A) receptor, which is a major inhibitory neurotransmitter receptor in the brain (Fritschy, 2008). Elevated E/I ratio associated with exaggerated excitatory glutamate signaling has also been implicated in Fragile X syndrome, a major heritable cause of intellectual disability and autism (Repicky et al., 2009).

Interestingly, a reduction of GABAergic signaling (the major inhibitory signaling in the adult brain) has been linked to neurodevelopmental disorders in multiple studies (Gogolla et al., 2009; Ma et al., 2005; Collins et al., 2006; Lionel et al., 2013). Noncoding single nucleotide polymorphisms within GABA receptor subunit genes have been associated with autism patients (Ma et al., 2005; Collins et al., 2006). *De novo* mutations in GABA receptor scaffolding protein gephyrin have been implicated in risk for autism, schizophrenia, and seizures (Lionel et al., 2013). In addition, postmortem studies revealed that GABA signaling proteins, such as GAD 65 and GAD 67, enzymes that normally facilitate GABA synthesis, are reduced in autistic brain (Fatemi et al., 2002). Down-

regulation of $GABA_A$ receptors was also found in brains of subjects with autism (Fatemi et al., 2009). These findings suggest that reduction of GABAergic signaling, which contributes to elevated E/I balance, is a widespread phenomenon found in multiple neurodevelopmental disorders.

Curiously, mutations of genes that normally sculpt and maintain E/I balance result in multiple, often comorbid, neurodevelopmental disorders, including autism, schizophrenia, intellectual disability and epilepsy (Herbert, 2011; Ting et al., 2012; Verpelli and Sala, 2012). *SYNGAP1* haploinsufficiency, as mentioned above, causes intellectual disability, autism, which always comorbid with epilepsy (Hamdan et al., 2009; Krepischi et al., 2010; Hamdan et al., 2011; Klitten et al., 2011; Zollino et al., 2011; Berryer et al., 2013).

Because of the important role of *SYNGAP1* in multiple neurodevelopmental disorders, animal models have been utilized to gain a deeper understanding of *SYNGAP1* function. *Syngap1* heterozygous (het) mice that model human *SYNGAP1* haploinsufficiency were created using gene-targeting techniques (Kim et al., 2003). In a recent mouse study, *Syngap1* haploinsufficiency was shown to disrupt E/I balance and information processing in the mouse brain (Clement et al., 2012). Signal propagation through the medial perforant path (MPP) of the dentate gyrus (DG), which is the major input pathway into the hippocampus, was monitored by laser photolysis of caged glutamate paired with fast voltage sensitive dye imaging. Signals originating in the DG of wild type (WT) mice were attenuated as they propagated through the circuit, but signals originating in the DG of het mice were amplified as they spread through

hippocampus, indicating that *Syngap1* haploinsufficiency disrupts information processing in the hippocampus, and also induced enhanced synaptic excitability (Clement et al., 2012). Thus, *SYNGAP1* plays an important role in normal neural behavior and cognition by maintaining E/I balance in the brain.

### ***SYNGAP1*** **plays an important role in neural apoptosis**

Mice homozygous for a *Syngap1* deletion die within first few days after birth (Knuesel et al., 2005). In order to study the function of *Syngap1*, the cre/loxP recombination system was used to create conditional knockout mouse mutants that could survive to post-natal stages (Knuesel et al., 2005). Syngap1 protein in these mutants exhibits a gradual loss beginning around first postnatal week, and reaches maximal loss at the third postnatal week (Knuesel et al., 2005). However, the degree to which *Syngap1* is lost varies among littermates. In a small population, Syngap1 levels were reduced to 20%-25% of wild type and they died at 2-3 postnatal weeks. In a larger group, Syngap1 levels remain more than 40% of wild type and these survived and remained healthy (Knuesel et al., 2005). To evaluate the consequences of Syngap1 reduction at post-natal stages, apoptotic cell death was quantified using an antibody to detect caspase-3 activity, an important degenerative enzyme activated during apoptosis (Rami et al., 2003). Activated caspase-3 antibody staining showed a significantly higher level of apoptosis in neurons of the hippocampus and cortex in these conditional *Syngap1* mutant mice than that in wild type, indicating that apoptosis is enhanced by reduction of Syngap1 and suggesting that *Syngap1* normally protects brain cells from apoptotic cell death (Knuesel et al., 2005). This study

may also provide an explanation for why *Syngap1* homozygous deletion is lethal to mice during early development.

Increased cell death also may indicate structural changes in the brain, or disruption of neural connectivity at early developmental stages by affecting early fundamental developmental processes (such as neuron proliferation, migration, and apoptosis), which leads to disrupted functions at later developmental stages. While these hypotheses are difficult to test in the mouse because of inaccessibility of embryonic stages, we hope to test these hypotheses in zebrafish (*Danio rerio*).

**A favored model to study mechanisms of human disorders – zebrafish (*Danio rerio*)**

Zebrafish (*Danio rerio*) is a small vertebrate tropical fish. It shares 75 – 80 % conservation with human genome, and around 70% of human disease genes (including *SYNGAP1*) have functional homologs in zebrafish (Langheinrich et al., 2003; Santoriello et al., 2012), which provides solid genetic basis for zebrafish to model human diseases.

Zebrafish has high fecundity and a single female can lay 200 – 300 eggs per week. The embryos are transparent and develop externally from the one-cell stage, which makes them easily to manipulate experimentally and easier to observe compared to the mouse, especially during embryonic stages (Santoriello et al., 2012).

In addition, stereotyped behaviors are determined early in developing zebrafish. A short period of alternating tail coiling appears at 17 hours post fertilization (hpf), response to touch starts at 21 hpf, and fish start to swim at 27 hpf (**Fig. 2**). All of these behaviors that initiate at early developmental stages corresponding to in utero stages of mouse provide a functional assay for the nervous system at early developmental stages in zebrafish. The cellular mechanisms of these behaviors were well understood (Brustein et al., 2003; Lambert et al., 2012; Kohashi et al., 2008), which allows us to directly test the functional consequences of genetic perturbations.

## Chapter 1: Effects of *syngap1* knockdown on early embryonic structure and global neural circuit functions

*SYNGAP1* haploinsufficiency has been linked to multiple neurodevelopmental disorders including autism, intellectual disability and epilepsy (Hamdan et al., 2009; Krepischi et al., 2010; Hamdan et al., 2011; Klitten et al., 2011; Zollino et al., 2011; Berryer et al., 2013). Recently, postmortem studies of human brain tissues have indicated a prenatal origin in etiology of neurodevelopmental disorders (Stoner et al., 2014; Miller et al., 2014; Voineagu et al., 2011). Specifically, defects of cortical patterning, which is normally established during embryonic stages, have been observed in the cortical regions of brains from individuals with autism (Stoner et al., 2014; Voineagu et al., 2011). Transcriptome analyses have revealed consistent changes in expression patterns of genes (including *SYNGAP1*) involved in neurodevelopmental disorders in prenatal brain of human patients (Miller et al., 2014; Voineagu et al., 2011). Informed by *SYNGAP1* haploinsufficiency and knockout studies in mouse, which suggest elevated E/I balance and increased apoptosis mechanisms (Clement et al., 2012; Knuesel et al., 2005) and human postmortem studies, which suggest a prenatal origin of brain disorders (Stoner et al., 2014; Miller et al., 2014; Voineagu et al., 2011), I used a morpholino strategy to knockdown *syngap1* in zebrafish to create a model to study the functional roles of *syngap1* at early embryonic developmental stages.

In this study, we used qPCR from a developmental RNA time-course of zebrafish embryos and show that both *syngap1a* and *syngap1b* are expressed

throughout development supporting the idea that they may play important functional roles in the early embryo. We then designed morpholinos to knock down either *syngap1a* or *syngap1b* in zebrafish. Knocking down either of the two zebrafish *syngap1a* and *b* duplicates caused similar morphological and behavioral phenotypes therefore for subsequent analyses, we focused our studies on *syngap1b*. We chose *syngap1b* because it is the dominant isoform at the developmental stages we used for analysis and Syngap1b protein sequence has a higher identity to human SYNGAP1 protein (NCBI BLAST score 1529 for Syngap1b versus 1149 for Syngap1a). Knockdown of *syngap1b* disrupted brain structures and increased cell death in brain and spinal cord, which can be rescued by injecting human *SYNGAP1* mRNA. These results highlight early developmental roles for *syngap1* in brain morphogenesis.

## Materials and Methods

### Fish maintenance

Adult wild-type and transgenic zebrafish were maintained in a recirculating Aquatic Habitats (Apopka, FL, USA) rack system at 28.5℃ on a 14:10 circadian light:dark cycle according to standard methods (Westerfield, 2000). Embryos and larvae were raised in a 28.5℃ incubator with the same 14:10 light:dark cycle and staged in hours post-fertilization (hpf). All experimental procedures in this dissertation were in accordance with National Institutes of Health (NIH) animal

care guidelines and have been approved by the University of Miami Institutional Animal Care and Use Committee (IACUC).

**qPCR developmental time course**

Total RNAs were extracted from a time courses of 2, 5, 8, 12, 15, 24, 36, 48, 72, 96, and 120 hpf zebrafish embryos using TRIzol reagent (Life Technologies, Carlsbad, CA, USA), 3 pools of 25 embryos were used for RNA extraction at each time point. Extracted RNA was treated with DNAase (Life Technologies, Carlsbad, CA, USA) by standard protocol. RNA was then used as template for qPCR using qScript One-Step SYBR Green qRT-PCR kit (Quanta Biosciences, Gaithersburg, MD, USA) to determine the developmental expression level of *syngap1a* and *b* with *ef1a* serving as an internal control. Primers (Integrated DNA Technologies, Coralville, IA, USA) for each gene were designed using primer3 (See **Table 1** for a list of these primers). Each PCR reaction contained: 1X One-Step SYBR Green Master Mix, 200 nM forward and reverse primer, 100 ng RNA template, 1X qScript One-Step RT and nuclease-free water to a final volume of 50 µL. The cycling conditions were: 48℃ for 10 min; 95℃ for 5 min; 40 cycles of 95℃ for 10s, 60℃ for 20s, and 72℃ for 45s; 72℃ – 95℃ for 20 min; 95℃ for 15s. Standard curves of both copies of *syngap1* and *ef1a* were made by replacing RNA template with purified standard PCR products using the same qPCR primer sets. Purification of PCR product was performed using Wizard® SV Gel and PCR Clean-Up System (Promega, Madison, WI, USA). Purified PCR products were quantified by NanoDrop (Thermo Scientific, Pittsburgh PA, USA). The absolute quantity of both *syngap1*

copies during development was calculated using methods described by Whelan et al (Whelan et al., 2003) and plotted using Excel (Microsoft, Redmond, WA, USA).

**Microinjections**

Antisense splice-modified morpholino oligonucleotides (MOs; Gene Tools, LLC., Philomath, OR, USA; **Table 2**) were designed against the common exon-intron boundaries based upon *syngap1a/b* variants annotated in the Ensembl database. Lyophilized MOs were rehydrated in nuclease-free water as 1 mM stored at 4℃. To ensure full resuspension of stored MOs, stock solutions were heated to 65℃ prior to making dilutions for injections. For injections, MOs were diluted with nuclease-free water to 0.5 mM, and colored with a tiny tip (touch 1% fast green with 10 µL tip without pipetting and add to morpholino solution) of 1% fast green for visualization, then injected into one-cell zygotes. To ensure that only successfully-injected embryos were further analyzed, a few hours after injection, embryos were sorted for even distribution of the green color throughout yolk and embryo. To find optimal dosage of MOs, I generated a dose-response curve by injecting a series of dosages (100 pL, 500 pL, 1 nL and 2 nL), and dilutions (0.5 mM, 500 pL) with highest behavioral effects and least morphological defects were used for morphological and behavioral analyses; dilution (0.5 mM, 100 pL) was used for cell death and rescue analysis.

To demonstrate gene specificity of phenotypes, the longest isoform of human *SYNGAP1* mRNA was transcribed using SP6 mMESSAGE Mmachine

RNA transcription Kit (Life technologies, Carlsbad, CA, USA). For rescue experiments, a total amount of 100-200 pg mRNA was injected into one-cell stage embryos, following with MOs injection (0.5 mM, 100 pL).

**RT-PCR and sequencing to validate MO knockdown**

RNA was harvested from 24 hpf embryos and larvae using TRIzol followed by DNAse treatment according to standard protocols (Life Technologies, Carlsbad, CA, USA). For cDNA synthesis, 1 µg of RNA was reverse transcribed using the SuperScript III™ First-Strand Synthesis System (Life Technologies). cDNA was then used as template for PCR to test for mis-splicing events induced by the MOs. Primers (Integrated DNA Technologies, Coralville, IA, USA) for each gene were designed using primer3. See **Table 2** for a list of these primers. Each PCR reaction contained: 1X GoTAQ hot start green master mix (Promega, Madison, WI), 2 µM forward and reverse primer, 50-60 ng of cDNA template and DNASE/RNASE free H2O to a final volume of 10 µL. The cycling conditions were: 95℃ for 2 min; 32 cycles of 95℃ for 30s, 55℃ for 30s, 72℃ for 1 min; 72℃ for 5 min and 4℃ for storage. PCR products were run on a 1% agarose gel and checked for banding patterns and relative band intensities (**Fig. 3**). Bands were gel-purified, and re-amplified for sequencing to determine how splicing was impacted by MO injections.

**Morphological and behavioral analysis**

For morphological comparison, images were captured on an Olympus D71 advanced micro-imager mounted on a Wild dissecting microscope. To analyze

morpholino induced behavioral phenotypes, high-speed videos were taken using a Fastcam 1024PCI (Photron USA Inc., San Diego, CA, USA). This camera was either mounted on a dissecting scope or, for FLOTE analysis, mounted with a Fujinon lens in a customized behavioral chamber. Parameters were as follows: shutter speed of 1/1000 (Advance Illumination; Rochester VT; Backlight LED Illuminator), 512 x 512 resolution, a frame rate of 250 f/s to assess swimming qualitatively and 1000 f/s to assess swimming kinematics. Three touch-evoked behaviors, elicited using a tungsten or fishing line probe, were recorded per individual. After capturing videos, Flote (Burgess and Granato, 2007) was used to quantitate changes in axis curvature over time and swimming velocity. The fishing line was used to elicit behaviors for Flote analysis to decrease the possibility of disrupting the tracking software.

**Acridine orange staining**

To analyze cell death in early zebrafish embryos, 28-30 hpf control embryos and *syngap1b* morphants were dechorionated and placed in 5 µg/ml of acridine orange (Sigma-Aldrich, St. Louis, MO, USA) for 30 minutes at 28.5℃. After staining, stained embryos were rinsed three times with system water. Then control embryos and morphants were anesthetized with 0.02% MS222 and mounted with 3% methylcellulose (Sigma-Aldrich, St. Louis, MO, USA). Images were captured on a Leica SP5 confocal microscope (Leica Microsystems, Wetzlar, Germany). Cell death was quantified with Fiji software: briefly, threshold of images was auto adjusted using “intermodes, B&W” mode; Midbrain, hindbrain

and spinal cord areas were selected manually and percentage of staining areas were measured automatically.

## Results

### Developmental expression pattern of *syngap1* in zebrafish

To determine the developmental expression patterns of *sygap1a* and *syngap1b*, I harvested RNA from eleven developmental stages ranging from 2 to 120 hpf and used gene-specific primers for one-step qPCR to determine developmental expression levels (**Fig. 4**). *syngap1a* transcript is expressed in cleavage-stage embryos, shows a significant level of maternally-derived mRNA, decreasing as the embryo gastrulates, and then increasing with embryo segmentation as early-born neurons exit the cell cycle and start to differentiate (Myers et al., 1986). *syngap1b* transcript levels are not dynamic during gastrulation but after 12 hpf show a similar expression profile to *syngap1a*. Based on these results, both transcripts are expressed in the early embryo. However, *syngap1b* is the dominant transcript expressed before 36 hpf, and *syngap1a* is the dominant transcript expressed after 36 hpf (**Table 3; Fig. 4**), indicating *syngap1b* functions primarily before hatching period while *syngap1a* functions majorly after hatching period. Expression levels are shown in **Table 3**, student t-test was performed between expression levels of both genes at each developmental stage (from 2 hpf to 120 hpf), and significance was shown in asterisks in **Fig. 4**.

### *Syngap1* morpholino-injected larvae (morphants) exhibit either unproductive swims with seizure-like behavior, or mortality

*Syngap1a* or *syngap1b* morpholino-injected animals exhibit behavioral phenotypes that include unproductive swims (typified with longer swim episode and decreased velocity; 68% of *syngap1a* morphants and 82% of *syngap1b* morphants) and in a subset of animals, seizure-like behavior (18%) (N=131 fish, **Fig. 5**), suggesting both copies function in the same neural circuit. In the normal swim response, each episode lasts for an average of 500 milliseconds, in contrast, each episode of seizure-like behaviors persists for several seconds, and is typified by a lack of coordinated movements (**Fig. 5**). Unproductive swimming also manifested as significantly decreased swimming velocity in *syngap1a/b* morphants compared with controls (**Fig.5**; N=8, $p<0.001$), indicating a less powerful swimming stroke and decreased motor capacity in *syngap1a/b* morphants. Behaviors were captured by high-speed cameras and are analyzed using FLOTE software (Burgess et al., 2007). Seizure-like behaviors are good indications of too much excitation in nervous system, which causes uncoordinated movements of fish.

### *Syngap1b* morphants exhibit absence of midbrain and hindbrain structure

In *syngap1b* morphants, the overall cross-sectional area of brain is smaller compared to control morpholino injected embryos (controls), brain ventricle is enlarged, midbrain-hindbrain boundary (the gap between posterior boundary of

midbrain and anterior boundary of hindbrain) is more compact, and hindbrain (the anterior boundary of hindbrain to the position of the first segment) is more condensed, and does not extend toward spinal cord as much as controls do. As a result, the spinal-hindbrain boundary is more rostral in *syngap1b* morphants (**Fig. 6**).

### ***Syngap1b*** **morphants exhibit increased cell death in brain and spinal cord**

To test for elevated cell death in morphants, I used acridine orange staining on both control embryos and morphants at 28-30 hpf. Staining areas were quantified for both control and *syngap1b* morphants by calculating the percentage of area in a z-projection of confocal images stained with acridine orange. In the midbrain, *syngap1b* morphants exhibited 5.5% area labeled with acridine orange (N=10 fish; SD=3.36) compared to 0.4% (N=10 fish, SD=0.29) in controls. In the hindbrain, *syngap1b* morphants exhibited 7.0% area labeled with acridine orange (N=10 fish; SD=2.61) compared to 0.5% (N=10 fish, SD=0.46) in controls. In the spinal cord, *syngap1b* morphants exhibited 30.0% area labeled with acridine orange (N=10 fish, SD= 14.76) compared to 2.0% in controls (N=10 fish, SD=1.26). There is an obvious increase in cell death in midbrain, hindbrain and spinal cord of *syngap1* morphants compared to control fish at 28-30 hpf (**Fig. 7**).

**Both disrupted brain structure and increased cell death in morphants could be rescued by human *SYNGAP1* mRNA**

Since both abnormal brain morphology and cell death are common off-target effects caused by morpholino and si-RNA knockdown technology (Robu et al., 2007), I used human *SYNGAP1* mRNA to attempt to rescue these phenotypes and thus test whether phenotypes were gene-specific. Importantly, both disrupted brain structure and increased cell death in *syngap1* morphants could be rescued by human *SYNGAP1* mRNA (**Fig. 7**): compared with *syngap1* morphants, staining areas of rescued fish were down to 3.3% (N=10 fish, SD=2.41), 2.7% (N=10 fish, SD=2.46) and 9.2% (N=10 fish, SD=5.09) for midbrain, hindbrain and spinal cord respectively. This result indicates that both abnormal brain structures and increased cell death in morphants are specifically caused by reduction of *syngap1* expression.

## Discussion

In this study, we successfully knocked down zebrafish *syngap1b* transcript by using morpholino knockdown strategy, which we utilized as a tool to perform functional study of *syngap1* (**Fig. 3**). Similar to previous mouse *Syngap1* heterozygous model (Clement et al., 2012), zebrafish *syngap1* morphants also exhibit abnormal behavior such as seizure-like behavior (**Fig. 5**). In addition, seizure-like behaviors are good indications of excessive excitation in nervous

system, which is another similarity to *Syngap1* heterozygous mouse model (Clement et al., 2012).

Our qPCR study indicates that both *syngap1* transcripts are expressed in the early embryo. Expression of *syngap1* hasn't been characterized in early embryonic stages, and this will be the first study to reach the early stages. Additionally, more evidence has shown that duplicates of genes in zebrafish are due to complementary loss of subfunctions (Lynch et al., 1999), such as *engrailed* genes in zebrafish: one is expressed in the pectoral appendage bud, while the other is expressed in hindbrain/spinal cord (Force et al. 1999); likewise, similar patterns exist in two *Notch* duplicates (Westin and Lardelli 1997) and two *Pax6* duplicates (Normes et al. 1998). However, *syngap1* duplicates in zebrafish suggest minimal sub functionalization since knockdown of either gene produces phenotypes.

Knockdown of *syngap1b* disrupts brain structures of zebrafish, suggesting a critical functional role of *syngap1* in zebrafish brain morphogenesis (**Fig. 6**). Underlying the structural defects, acridine orange staining shows that reduction of syngap1b increases cell death in zebrafish brain and spinal cord (**Fig. 7**). Cell death can be rescued by co-injecting human *SYNGAP1* mRNA, indicating disrupted brain structures and behaviors in morphants are specifically caused by reduction of syngap1 in zebrafish (**Fig. 7**).Our findings in zebrafish are consistent with mouse study in which increased neuronal apoptosis was observed in the hippocampus, cerebellum and cortex of *Syngap1* knockout mice by the first postnatal day (Knuesel et al., 2005). Combined with our finding in this study,

which focuses on earlier embryonic stages, we can conclude that increased neuronal death in the brain is a common endophenotype specifically caused by reduction of Syngap1 protein at early embryonic stages. Elevated neuronal death could also be a potential mechanism that explains disruption of brain structures and abnormal behaviors in later development. Therefore, we speculate that *syngap1* plays important roles in brain morphogenesis and behaviors by regulating neuronal apoptosis.

Data in this chapter validates the effectiveness of the zebrafish *syngap1* heterozygous model. In previous mouse *Syngap1* heterozygous model, it has been demonstrated that premature glutamatergic synapses shifted E/I balance toward aberrant excitation (Clement et al., 2012). Elevated E/I balance was again shown as an important phenomenon in neurodevelopmental disorders associated with *syngap1* haploinsufficiency in zebrafish model since these models also exhibited seizure-like activity. Additionally, increased neuronal death caused by Syngap1 reduction has been demonstrated as a common endophenotype throughout early embryonic development. What's more, elevated E/I balance due to reduction of GABAergic signaling has been proposed as a potential mechanism of neurodevelopmental disorders such as ASD, schizophrenia, and seizures in multiple studies (Gogolla et al., 2009; Ma et al., 2005; Collins et al., 2006; Lionel et al., 2013). Our unpublished data has shown dramatic delays in the differentiation of both GABAergic and glutamatergic neurons in the mid and hindbrain (Robert Kozol). In order to explore the potential cellular mechanisms of abnormal functions caused by *Syngap1*

haploinsufficiency, I have decided to utilize the *dlx6a-1.4kbdlx5a/dlx6a:GFP* transgenic zebrafish line, in which GABA precursors are labeled by GFP (Yu et al., 2011), to preform further studies.

## Chapter 2: Effects of *syngap1* knockdown on early proliferation, migration and apoptosis of GABAergic neuron precursors

Increased E/I balance due to reduction of GABAergic signaling has been proposed as a potential mechanism of neurodevelopmental disorders such as ASD, schizophrenia, and seizures in multiple studies (Gogolla et al., 2009; Ma et al., 2005; Collins et al., 2006; Lionel et al., 2013). Based on our findings of morphological and behavioral changes in zebrafish *syngap1* morphants, I hypothesized that GABAergic signaling is reduced in *syngap1* morphants as a result of early disruption of GABAergic neuronal precursors: there would be fewer GABAergic neurons in morphants which could result from fewer cell divisions, failure of GABAergic neuron precursors to migrate properly, or increased cell death in GABAergic neuronal precursors. To test this hypothesis, I used *dlx6a-1.4kbdlx5a/dlx6a:GFP* transgenic zebrafish line, in which regulatory sequences for the Dlx5a and Dlx6a transcription factors drive the expression of GFP, to visualize these GABA precursors (Yu et al., 2011).

In *dlx6a-1.4kbdlx5a/dlx6a*:*GFP* transgenic line, telencephalic interneurons migrate from the ventral to the dorsal telencephalon, an event which is conserved in all vertebrates (Marin et al., 2001; Metin et al., 2006) and can be visualized during zebrafish forebrain development (Mione el al., 2008) (**Fig. 8**). Therefore, in this chapter I use the *dlx6a-1.4kbdlx5a/dlx6a*:*GFP* transgenic line as a powerful platform to study proliferation, migration and apoptosis of GABAergic precursors.

## Materials and methods

### Analysis of GABA precursor cell numbers

GFP positive controls and *syngap1b* morphants were sorted for fluorescence and dechorionated around 21 hpf. Prior to fixation, larvae were anesthetized on ice for 30 minutes. The water was then replaced with 4% paraformaldehyde (PFA) diluted from 16% stock (Pierce Protein Biology Products, Rockford, IL, USA) in 1 X phosphate buffer solution (PBS). Sorted fish were fixed with 4% PFA at room temperature for 1h at 22 hpf, 24 hpf and 28 hpf. Samples were washed three times with 1 X PBS, deyolked and mounted in 1 X PBS on coverslips for imaging. Single-cell resolution images were captured on a confocal microscope Leica SP5 (Leica Microsystems, Wetzlar, Germany) with 20 X objective, 2 µm Z-step and 1024 X 1024 resolution. Image analysis was performed using Fiji software: neurons were color coded in depth using Z code stack plugin, and counted with ITCN plugin, both from Fiji official website. Neurons were counted manually to double check the accuracy

### Cell apoptosis analysis

For analysis of apoptosis, both control and morpholino-injected embryos were fixed with 4% PFA (Pierce Protein Biology Products, Rockford, IL, USA) at 22 hpf, 24 hpf and 28 hpf at room temperature for 1h. Wash with PBS-0.5% Tween-20 (PBST) for 5 minutes (min) three times, treated with acetone (VWR, Radnor, PA, USA) for 7 min at -20 $^{o}$C, two washes with PBST-1% DMSO (VWR,

Radnor, PA, USA) (PBST-DMSO) for 15 min. Embryos were blocked for 1h with 5% donkey serum (Sigma, St. Louis, MO, USA), 1% BSA (Sigma, St. Louis, MO, USA) in PBST-DMSO at room temperature. Embryos were incubated with anti-active caspase 3 antibody (1:500; Abcam, Cambridge, MA, USA) overnight at 4 $^{o}$C. Embryos were washed twice with PBST-DMSO for 10 min each. Embryos were incubated in secondary antibody goat-anti-rabbit 568 antibody (1:1000; Life technologies, Grand Island, NY, USA) for 2h at room temperature. Embryos were washed twice with PBST-DMSO for 10 min each. Embryos were then mounted on coverslips and imaged. Image analysis was performed using Fiji software: neurons under apoptosis were quantified with ITCN plugin and apoptotic neurons were counted manually to double check the accuracy.

## Results

### GABAergic neuron precursors are reduced in *syngap1b* zebrafish morphants

The number of GABAergic neuron precursors in the brain was quantified, and a significant decrease of GABA precursors was observed at 22, 24 and 28 hpf. The reason we decided to focus on these three stages is that robust GFP expression was first observed in the telencephalon starting at 1 dpf as previously reported (Yu et al., 2011), and we expected to see mitosis of these progenitors at a stage earlier than 24 hpf. The reason to end at 28 hpf is because 28 hpf is the stage we studied for cell death and rescue, and it turns out to be an informative

stage. In order to quantify cell numbers as accurately as possible, confocal stack images were first color coded with depth, cells at three different depths were counted separately and then added up for analysis. The average number of GABA precursors at 22 hpf is: 314 in controls (N=8 fish, SD=54.8) and 198 in *syngap1b* morphants (N=8 fish, SD=38.4; $p<0.001$); at 24 hpf is: 322 in controls (N=8 fish, SD=95.1) and 238 in *syngap1b* morphants (N=8 fish, SD=81.5; $p<0.05$); at 28 hpf is: 371 in controls (N=8 fish, SD=85.3) and 208 in *syngap1b* morphants (N=8 fish, SD=22.0; $p<0.0001$).

**Apoptosis is increased in the areas of GABAergic neuron precursors in *syngap1b* zebrafish morphants**

To investigate the potential mechanism of reduction of GABAergic neuron precursors, I did active caspase-3 antibody staining on both controls and *syngap1b* morphants at 22, 24 and 28 hpf, and determined the number of neurons undergoing apoptosis in GABAergic neuron precursor area (**Fig. 10**).The number of neurons undergoing apoptosis in the GABAergic neuron precursor area (the minimal rectangular area which covers all GABA precursor neurons) is 10at 22 hpf (N=4 fish, SD=3.4) in controls and 46 (N=4 fish, SD=8.8; $p<0.001$) in *syngap1b* morphants; at 24 hpf, it is 7 (N=4 fish, SD=5.1) in controls and 43 (N=4 fish, SD=7.2; $p<0.0001$) in *syngap1b* morphants; and at 28 hpf, it is 5 (N=4 fish, SD=2.5) in controls and 43 (N=4 fish, SD=17.5; $p<0.001$) in *syngap1b* morphants.

## Discussion

In this chapter, we partially tested our hypothesis that GABAergic signaling is reduced in *syngap1* morphants as a result of early disruption of GABAergic neuronal precursors: we found a reduction of GABA precursors in syngap1 morphants at 22, 24 and 28 hpf; increased apoptosis in GABA precursor area may be responsible for this reduction.

The amplification patterns of GABA progenitors have changed from 22 hpf to 28 hpf: two GFP clusters of GABAergic precursor neurons were observed at 22 hpf, divided into four clusters at 24 hpf and started to merge as 2 larger clusters at 28 hpf (**Fig. 10**). Amplification pattern in *Syngap1b* morphants at 22 hpf looks very similar to amplification pattern in controls at 24 hpf (**Fig. 10 A & B**), indicating a precocious amplification pattern of GABA precursors in *syngap1b* morphants. This reminds us of the premature development of dendritic spine synapses in the *Syngap1* haploinsufficiency mouse model (Clement et al., 2012), suggesting precocity of GABA precursor amplification may be another phenotype caused by reduction of syngap1.

I also did anti-phospho-histone H3 (Ser10) staining on both controls and *syngap1b* morphants at 22, 24 and 28 hpf, however, I didn't see any overlap between staining and GFP, indicating that these GABA progenitors were divided at stages earlier than 22 hpf. This is consistent with a previous study that *dlx5* and *dlx6* are predominantly restricted to postmitotic, differentiating neurons in subventricular and mantle zones (Liu et al., 1997; Panganiban et al., 2002).

Since anti-phospho-histone H3 (Ser10) staining is troublesome for young embryos prior to 20 hpf, EdU staining would be a promising alternative to study proliferation of these GABA precursors. Since anti-capase-3 staining barely showed any overlap between GFP and staining, we would suspect apoptosis of these GABA precursors occur much at stages prior to 22 hpf, therefore EdU staining would also provide information on time points of birth and death of these GABA precursors. Further studies are needed to investigate cellular processes such as cell proliferation and cell migration. Then a more comprehensive explanation could be given as a potential mechanism of E/I imbalance.

## Discussion

In this study, we successfully generated a zebrafish *syngap1* heterozygous model using morpholino knockdown strategy, and for the first time, we show that the *syngap1* gene plays functional roles at embryonic stages. This embryonic perspective complements previous mouse *Syngap1* haploinsufficiency and *Syngap1* knockout studies, which focused on postnatal developmental stages (Clement et al., 2012; Clement et al., 2013; Knuesel et al., 2005). Our findings support the emerging view that largely comes from post-mortem studies of human brain tissue of a prenatal origin in etiology of neurodevelopmental disorders associated with ASD (Stoner et al., 2014; Miller et al., 2014; Voineagu et al., 2013). The initiative to study the functional roles of *syngap1* was motivated by increasing human patient data associated with *SYNGAP1* haploinsufficiency (Hamdan et al., 2009; Krepischi et al., 2010; Hamdan et al., 2011; Klitten et al., 2011; Zollino et al., 2011; Berryer et al., 2013). The behavioral similarities (seizures) among human patients, mouse and zebrafish syngap1 haploinsufficiency models indicate a conserved role of *syngap1* among three organisms. Our qPCR data suggests *syngap1* functions in early embryonic stages, plus the advantages of zebrafish to study embryonic stages. These motivate us to further investigate the functional roles of *syngap1* in zebrafish.

Seizure-like behaviors are convincing indications of disrupted E/I balance in the nervous system, and seem to be a common phenotypes caused by *SYNGAP1* haploinsufficiency from multiple models: In human patients with

*SYNGAP1 de novo* mutations, epilepsy is commonly comorbid with autism and intellectual disability (Berryer et al., 2013; Hamdan et al., 2011). In mouse *Syngap1* haploinsufficiency model, mutant mice exhibit seizure behavior and elevated synaptic E/I balance has been detected (Clement et al., 2012). Because of the E/I imbalance studies and previous GABA signaling studies (Gogolla et al., 2009; Ma et al., 2005; Collins et al., 2006; Lionel et al., 2013), we are motivated to investigate the cellular mechanism underlying E/I imbalance. We found that a significant reduction of GABAergic neuronal precursors at 22 – 28 hpf, which can be a potential mechanism that causes elevated E/I balance. We also found an increased apoptosis in the area of GABAergic neuronal precursors, which may be an explanation to the reduction of GABA precursors. We suspect that E/I imbalance could possibly be caused by a multitude of cellular processes in addition to apoptosis, such as disrupted proliferation, disrupted migration, which needs further investigation.

Disruption of midbrain and hindbrain structures in *syngap1* zebrafish morphants was another common phenotype caused by reduction of Syngap1 expression. In addition, rescuable cell death indicates that *syngap1* knockdown specifically causes increased neuron apoptosis in midbrain and hindbrain, which is a consistent phenotype as discovered in the *Syngap1* knockout mouse model (Knuesel et al., 2005). The midbrain-hindbrain boundary (MHB), where the isthmic organizer is located, is a conserved signaling center in the brain among vertebrates. Signals, such as FGF8 and WNT1, emanating from the MHB act to establish neural identities within the brain (Rhinn et al., 2001; Raible et al., 2004;

Dworkin et al., 2013). When this signaling is disrupted, one of the common phenotypes is apoptosis. Apoptosis is one of the signatures of failure to maintain MHB: ectopic cell death has been detected in several mouse mutant lines, including *Fgf8* knockout mutant, *Wnt1* $^{-/-}$ and *En1*$^{-/-}$ mutants; ectopic cell death is the major cause of deletion of midbrain and cerebellum brain structures (Chi et al., 2003; Dworkin et al., 2012; Sgado et al., 2006; Alavian et al., 2009). In addition, loss of *Grhl2b* in mouse causes increased apoptosis in MHB, which can be rescued by *Eng2a*, which is a direct target gene of *grhl2b* in the MHB (Dworkin et al., 2012). Previous studies have also demonstrated that *Eng2a* is critical for cell survival (Sgado et al., 2006; Alavian et al., 2009). Interestingly, *Grhl2b* acts with *Fgf8* in MHB patterning and morphogenesis (Dworkin et al., 2012), indicating that *Grhl2b* functions within *Fgf8* signaling pathway. Therefore, the similarity between phenotypes of *syngap1* zebrafish morphants and mouse mutants discussed above shows that both *syngap1* in zebrafish and *fgf8* signaling pathway in mouse play critical roles in MHB maintenance and morphogenesis. What's more, FGF signaling can lead to the initiation of Ras/ERK pathway (Dorey and Amaya, 2010), and *syngap1* can inactivate Ras protein by its RasGAP domain. This similarity between *fgf8* and *syngap1* motivates us to consider the possibility that *syngap1* and *fgf8* may work together in a signaling pathway important for brain morphogenesis, which would be an interesting direction for future research.

The zebrafish model we created using morpholino knockdown turns out to be very effective and informative in terms of studying embryonic cellular,

molecular and morphologic processes. However, one common problem of morpholino strategy is the effect of morpholinos lasts only the first few days of development (up to 5 days) (Bill et al., 2009), making it unstable to study gene functions at later developmental stages, which would correspond to long-term phenotypes of neurodevelopmental disorders caused by prenatal dysfunction. Therefore, in future studies, it will be critical to establish a stable *syngap1* zebrafish mutants. Several promising genome editing technologies have been developed to successfully create stable mutants in zebrafish over the past few years, such as Zinc finger nuclease (ZFN), TAL-effector-nucleases (TALENs) and Clustered Regularly Interspaced Short Palindromic Repeats/CRISPR-associated system (CRISPR-Cas) (Foley et al., 2009; Grunwald et al., 2013; Chang et al., 2013; Hwang et al. 2013). Stable mutants will allow us to investigate roles of candidate disease genes such as *SYNGAP1* throughout neural circuit development and it will bridge the current gap between early development and the phenotypes that are used to diagnose neurodevelopmental disorders.

## Figures

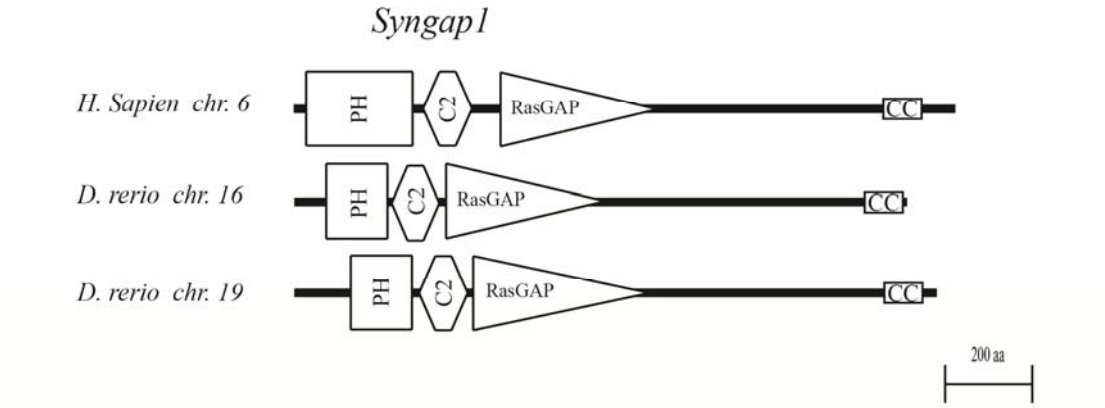


**Figure 1.** Illustration of conserved functional domains of SYNGAP1 in human and zebrafish (courtesy of Robert Kozol)**.** In human, there is one copy of *SYNGAP1* gene on chromosome 6. In zebrafish, there are two copies of *syngap1* due to genome duplication: one of these copies is on chromosome 16, *syngap1b*; the other is on chromosome 19, *syngap1a*. Functional domains of SYNGAP1 are conserved between human and zebrafish, both include pleckstrin homology (PH) domain; C2 domain; Ras GTPase-activating proteins (RasGAP) domain; and coiled coil (CC) domain.

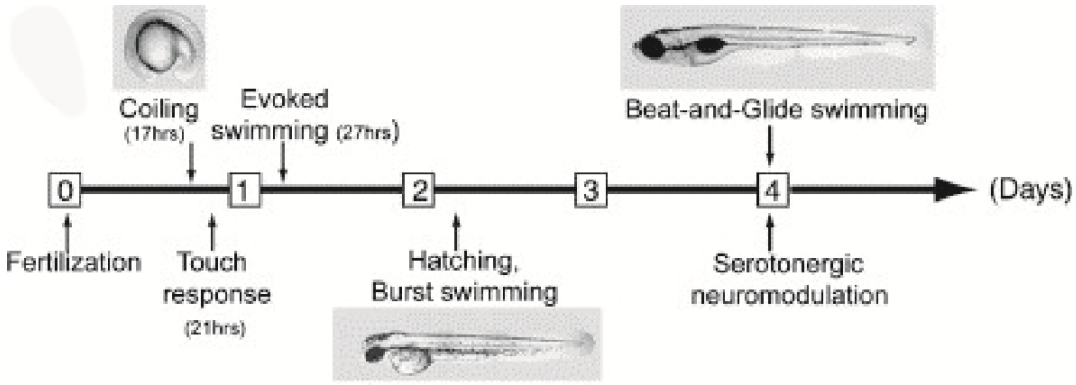


**Figure 2.** The chronological sequence of the appearance of stereotyped motor behaviors during zebrafish development. Images emphasize key motor behaviors before and after hatching (~52 hpf) of zebrafish (Adapted from Brustein et al., 2003).

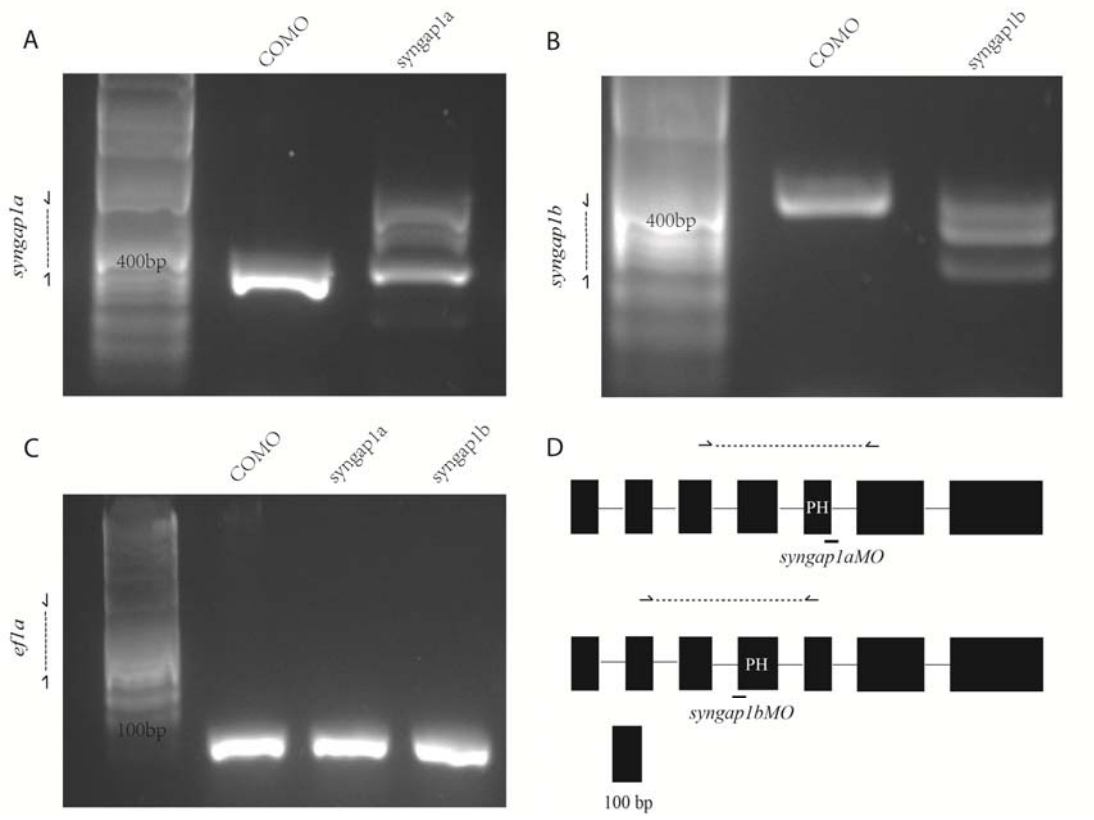


**Figure 3.** Zebrafish *syngap1* morpholino design and validation. (A-C) RT-PCR validation of morpholino knockdown. (A) Injection of *syngap1a* MO reduced the level of wild type *syngap1a* expression and produced three larger *syngap1a* MO-specific bands due to intron retention. (B) Injection of *syngap1b* MO reduced the level of wild type *syngap1b* expression and produced a partial exon deleted band due to exon skipping. (C) Neither injection of *syngap1a* or *syngap1b* MO reduced the level of wild type *ef1a* (internal control) expression. (D) Illustration of position of designed morpholinos for both *syngap1a* and *syngap1b* genes. Only seven of the Syngap1 exons are depicted. The *syngap1a* MO targets the exon 5/intron 5 splice-junction of the *syngap1a* gene. The *syngap1b* MO targets the intron 3/exon 4 splice-junction of the *syngap1b* gene. Based upon sequencing morphant-specific bands, both *syngap1a* and *syngap1b* MOs would be predicted to truncate the corresponding syngap1 protein in the plekstrin homology domain. Black blocks indicate exons while straight lines indicate introns; Arrows represent positions of diagnostic primers.

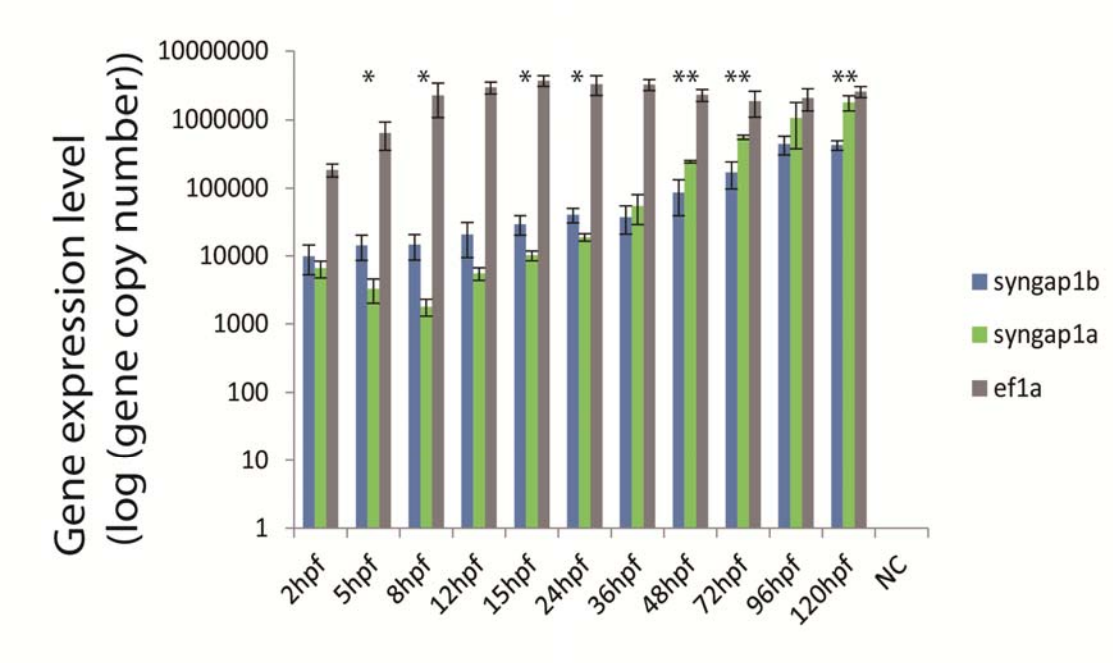


**Figure 4.** Developmental expression pattern of *syngap1* in zebrafish. Combined developmental expression patterns of *syngap1a* and *syngap1b* from 2 hpf to 120 hpf; Y axis stands for gene expression level, represented by log scale of gene copy number. Gene copy number was calculated based on the standard curve method with absolute copy number determined by weight of initial template and size of PCR product. Error bar is standard deviation. Asterisks indicate there is a significant difference in expression level between *syngap1a* and *syngap1b* at that stage. Statistical significance: * $p<0.05$, ** $p<0.01$.

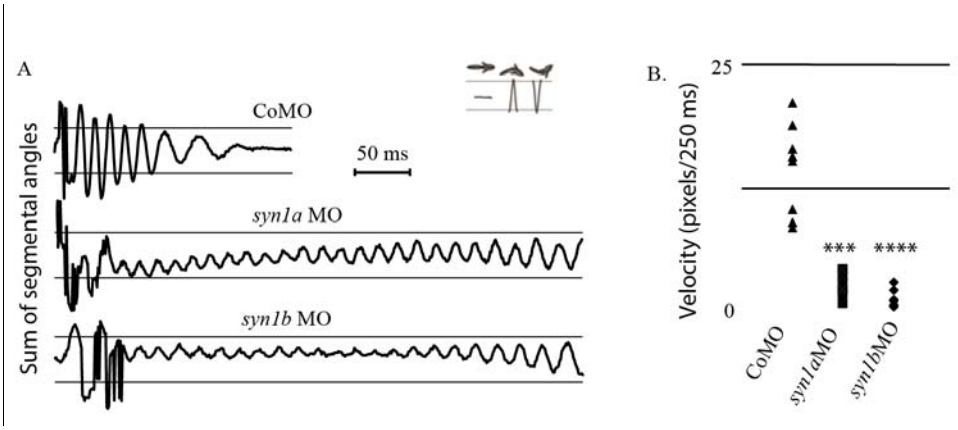


**Figure 5.** Knocking down *syngap1* disrupts swim responses in three day-old larvae (courtesy of Robert Kozol). (A) Angle of curvature is plotted versus time for representative swim responses. All plots are to the same scale with horizontal lines for reference. Morphants show a longer swimming episode which is typified by a lack of coordinated movements. (B) Quantification of swimming episode velocity. Morphants exhibit a significantly slower swimming response than controls. Statistical significance: *** p<0.001, **** p<0.0001.

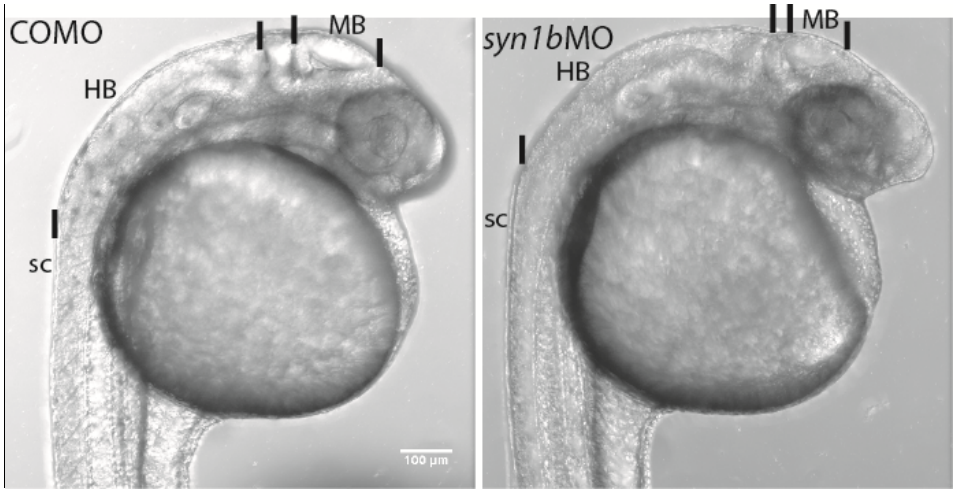


**Figure 6.** Reduced size of midbrain and hindbrain in *syngap1b* morphants at 28 hpf. Abbreviations in this figure: Hindbrain (HB), Midbrain (MB), Spinal Cord (SC). Midbrain and hindbrain boundary (MHB) is the gap between posterior boundary of midbrain and anterior boundary of hindbrain. Size of hindbrain is measured from the anterior boundary of hindbrain to the position of the first segment.

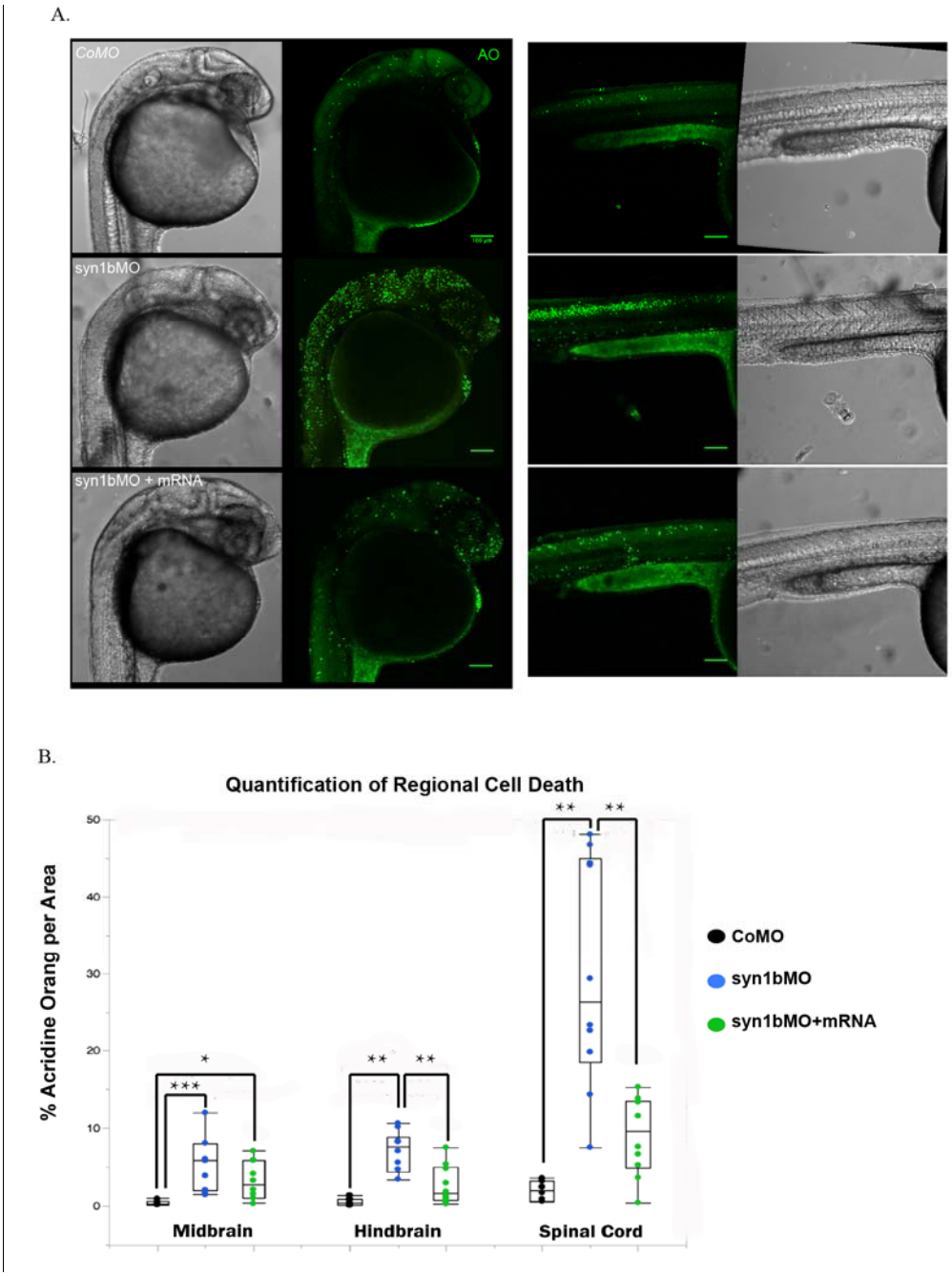


**Figure 7.** Rescuable cell death in the brain and spinal cord of zebrafish *syngap1b* morphants. (A) Acridine orange staining on controls, *syngap1b* morphants and rescued embryos at 28 hpf. (B) Quantification of AO stained area in midbrain, hindbrain and spinal cord. Data was analyzed using a one-way ANOVA with a post-hoc means comparison and bonferroni correction. Asterisks indicate significance values for means comparison, * $p<0.016$, ** $p<0.001$, *** $p<0.0001$ (Table 4, Table 5). Scale bars: 100 μm.

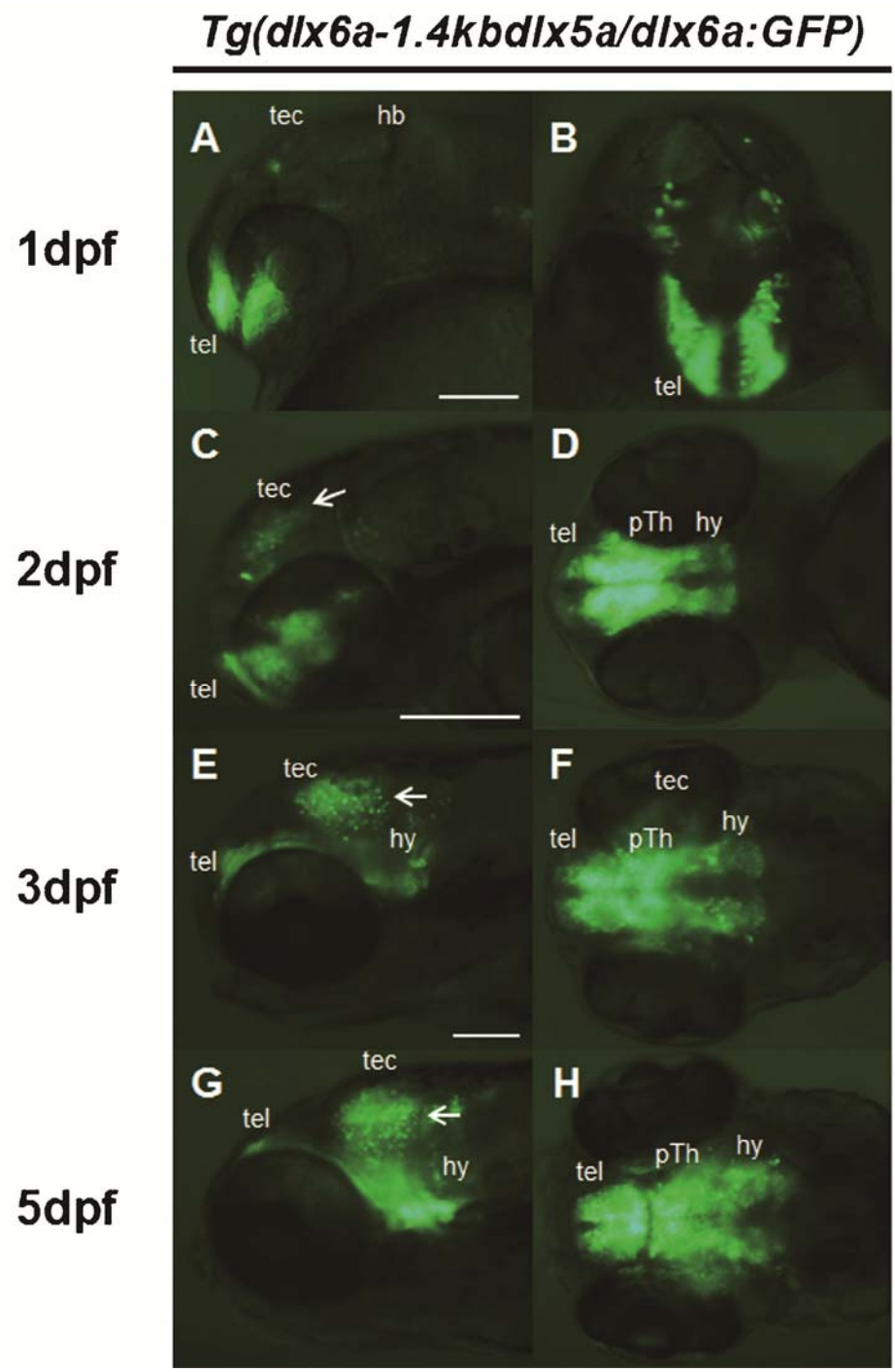


**Figure 8.** GFP reporter gene expression patterns in the *dlx6a-1.4kbdlx5a/dlx6a:GFP* live embryos. (A-B) robust GFP expression is first found in the telencephalon starting at 1 dpf. (C-H) GFP expression in the ventral diencephalon (prethalamus and hypothalamus) appears at ~2 dpf and becomes more apparent after 3 dpf. Arrows: scattered populations of GFP-positive cells are also clearly identified in the midbrain tectum. (A, C, E, and G): lateral views, anterior to the left, dorsal up; (B): dorsal views, anterior down; (D): ventral views, anterior to the left; (F and H): dorsal views, anterior to the left. Scale bars: 50 μm (A and B) and 100 μm (C–H). *Abbreviations*: hb, hindbrain; pTh, prethalamus; hy: hypothalamus; tec, tectum; tel, telencephalon. (Adapted from Yu et al., 2011).

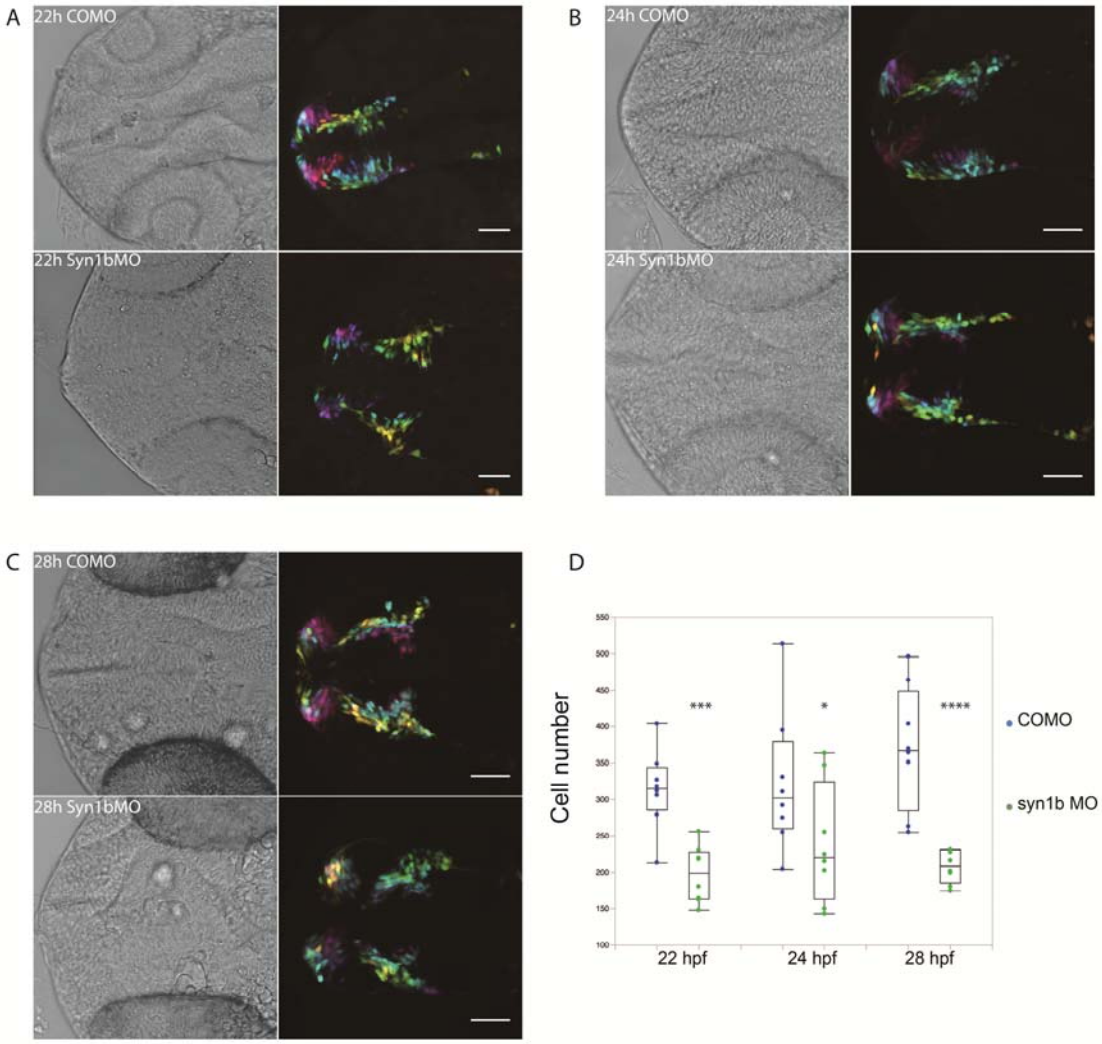


**Figure 9.** Reduction of GABAergic neuron precursors in zebrafish *syngap1b* morphants at 22, 24, and 28 hpf. (A-C) Color-coded images of GABAergic neuron precursors in zebrafish *syngap1b* morphants at 22, 24, and 28 hpf. Dorsal view, anterior to the left. GABA precursors were color coded in depth, color code scale from surface to deeper into the tissue is: orange – yellow – green – blue – purple – magenta - pink – red. (D) Quantification of number of GABA precursors in both controls and *syngap1b* morphants at 22, 24 and 28 hpf. Statistical significance: * $p<0.05$, ** $p<0.01$, *** $p<0.001$, **** $p<0.0001$. Scale bars: 50 μm.

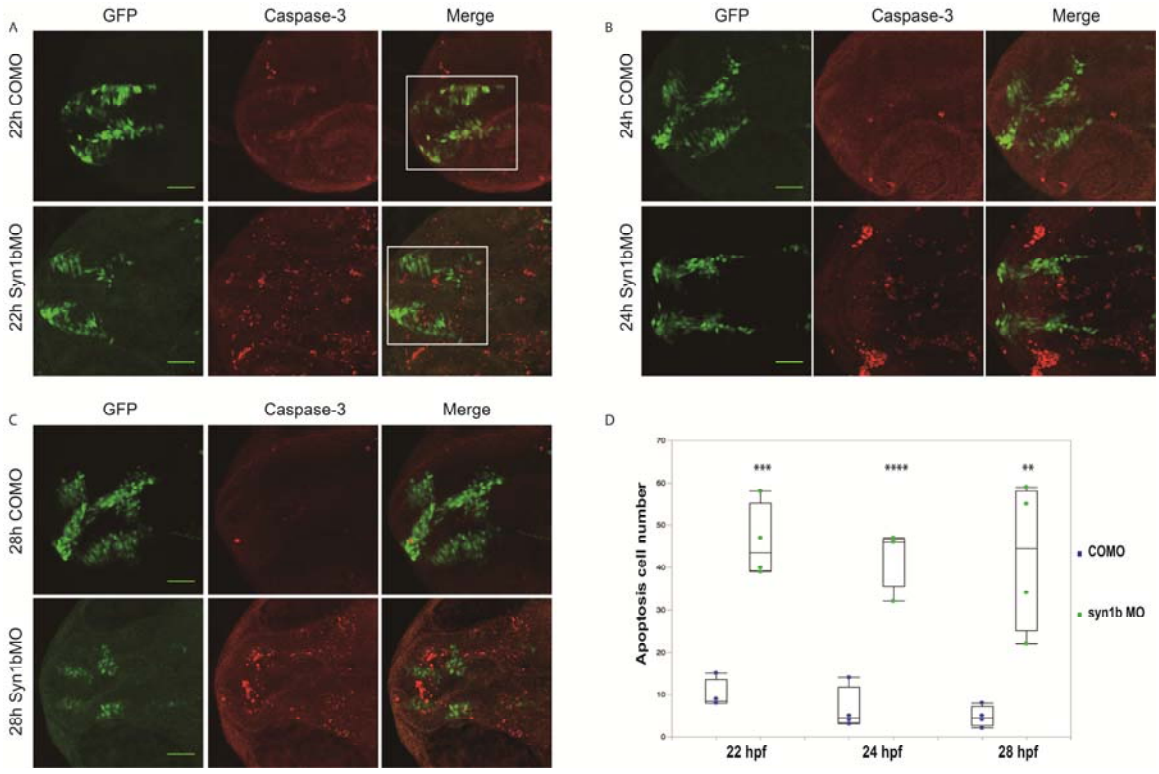


**Figure 10.** Increased apoptosis in GABAergic neuron precursors areas in zebrafish *syngap1b* morphants at 22, 24, and 28 hpf. (A-C) Images of GABAergic neuron precursors (Green) and caspase-3 antibody staining (Red) in zebrafish *syngap1b* morphants at 22, 24, and 28 hpf. Dorsal view, anterior to the left. (D) Quantification of number of apoptosis cells in both controls and *syngap1b* morphants at 22, 24 and 28 hpf. Statistical significance: * $p<0.05$, ** $p<0.01$, *** $p<0.001$, **** $p<0.0001$. White rectangel represents GABA precursor area. Scale bars: 50 µm.

## Tables

**Table 1**. Lists of primers used for qPCR.

| Gene | Oligonucleotide (5' - 3') |
|---|---|
| *syngap1a* | CGAACCCTCACGCTCATC<br>AACTCATTCATGAAGCCCAGA |
| *syngap1b* | GACGACAGATCTCCATGCAC<br>GAGGAGTGGCGAGAGATGAA |
| *ef1a* | CTGGAGGCCAGCTCAAACAT<br>ATCAAGAAGAGTAGTACCGCTAGCA |

**Table 2**. Sequences of antisense splice-site targeted **morpholino** oligonucleotides and diagnostic PCR primers.

| Gene | Chr. | Target | Sequence | Ensembl |
|---|---|---|---|---|
| *syngap1a* | 19 | ex5/in5 | **AGCACCTCGAAGCAGTACTCCTGGC** | ENSDARP: 00000087800 |
| | | ex3 | TACACAGCCATTTCGACAGC | |
| | | ex6 | GCTGCAGATTCTCGATCCAT | |
| *syngap1b* | 16 | in3/ex4 | **TCCTGTGAGGGAGCAATAACAGCAT** | ENSDARP: 00000087797 |
| | | ex2 | CATGGAGATCCCACCCACT | |
| | | ex5 | TTGGGTTTGACAGCTCTCTG | |

**Table 3.** Absolute quantification of *syngap1a*, *syngap1b* and *ef1a* from 2 hpf to 120 hpf.

| Stages | Gene copy number of *syngap1a* | Standard Deviation | Gene copy number of *syngap1b* | Standard Deviation | Gene copy number of *ef1a* | Standard Deviation |
|---|---|---|---|---|---|---|
| 2 hpf | 6572.409 | 1812.32 | 9820.222 | 4570.183 | 185794.3 | 39234.13 |
| 5 hpf | 3283.672 | 1266.593 | 14291.12 | 5774.832 | 642602.3 | 282030.1 |
| 8 hpf | 1794.983 | 497.4747 | 14591.39 | 5931.473 | 2237701 | 1150946 |
| 12 hpf | 5542.143 | 1172.891 | 20494.54 | 11064.2 | 2928261 | 590756.2 |
| 15 hpf | 10175.46 | 1667.123 | 29813.24 | 9787.704 | 3685538 | 665749.2 |
| 24 hpf | 18807.27 | 2369.808 | 40859.73 | 9670.574 | 3273872 | 1047815 |
| 36 hpf | 55098.19 | 25830.29 | 37847.58 | 16982.21 | 3211841 | 592074.6 |
| 48 hpf | 244344.1 | 9013.557 | 86360.76 | 46990.72 | 2271972 | 448164.3 |
| 72 hpf | 558013.6 | 37701.47 | 169737.8 | 72359.89 | 1838938 | 741791 |
| 96 hpf | 1064893 | 688072.7 | 442224.2 | 133176.7 | 2056015 | 730095 |
| 120 hpf | 1764645 | 434147.2 | 426676.8 | 65677.99 | 2531975 | 451818.4 |

**Table 4.** Statistical results for *syngap1b* morphants cell death - ANOVA.

| Source | | df | Sum of Squares | Mean Square | F | Sig. (p<) |
|---|---|---|---|---|---|---|
| Midbrain | Between Subjects | 2 | 131.5 | 65.8 | 11.5 | 0.0003 |
| | Within Subjects | 27 | 154.7 | 5.7 | | |
| | Total | 29 | 286.2 | | | |
| Hindbrain | Between Subjects | 2 | 220.8 | 110.4 | 25.3 | 0.0001 |
| | Within Subjects | 27 | 117.7 | 4.4 | | |
| | Total | 29 | 338.5 | | | |
| Spinal Chord | Between Subjects | 2 | 4254 | 2127 | 26.0 | 0.0001 |
| | Within Subjects | 27 | 2208 | 81.8 | | |
| | Total | 29 | 6462 | | | |

**Table 5.** Paired t-test for *syngap1b* morphants cell death.

| | Midbrain | Hindbrain | Spinal Cord |
|---|---|---|---|
| CoMO **vs** *syngap1b* MO | p<0.0001 | p<0.0001 | p<0.0001 |
| *syngap1b* MO **vs** MO + *SYNGAP1* mRNA | n.s. | p<0.0001 | p<0.0001 |
| CoMO **vs** MO + *SYNGAP1* mRNA | p<0.016 | n.s. | n.s. |

## References


Alavian, K. N., P. Sgado, L. Alberi, S. Subramaniam, and H. H. Simon. "Elevated P75ntr Expression Causes Death of Engrailed-Deficient Midbrain Dopaminergic Neurons by Erk1/2 Suppression." *Neural Dev* 4 (Mar 2009): 11.

Axelrad , D., Adamas K., …, Weber K. "Neurodevelopmental Disorders." *America's Children and the Environment* 3, (Jan 2013): 311-340.

Bavelier, D., D. M. Levi, R. W. Li, Y. Dan, and T. K. Hensch. "Removing Brakes on Adult Brain Plasticity: From Molecular to Behavioral Interventions." *J Neurosci* 30, no. 45 (Nov 2010): 14964-71.

Berryer, M. H., F. F. Hamdan, L. L. Klitten, R. S. Moller, L. Carmant, J. Schwartzentruber, L. Patry*, et al.* "Mutations in Syngap1 Cause Intellectual Disability, Autism, and a Specific Form of Epilepsy by Inducing Haploinsufficiency." *Hum Mutat* 34, no. 2 (Feb 2013): 385-94.

Bill, B. R., Petzold A. M., Clark K. J., Schimmenti L. A., Ekker S. C. "A Primer for Morpholino Use in Zebrafish." *Zebrafish* 6, no. 1 (Mar 2009): 69-77.

Brustein, E., L. Saint-Amant, R. R. Buss, M. Chong, J. R. McDearmid, and P. Drapeau. "Steps During the Development of the Zebrafish Locomotor Network." *J Physiol Paris* 97, no. 1 (Jan 2003): 77-86.

Burgess, H. A., and M. Granato. "Sensorimotor Gating in Larval Zebrafish." *J Neurosci* 27, no. 18 (May 2007): 4984-94.

Chang, N., C. Sun, L. Gao, D. Zhu, X. Xu, X. Zhu, J. W. Xiong, and J. J. Xi. "Genome Editing with Rna-Guided Cas9 Nuclease in Zebrafish Embryos." *Cell Res* 23, no. 4 (Apr 2013): 465-72.

Chen H.J., Rojas-Soto M., Oguni A., Kennedy M.B. "A Synaptic Ras-GTPase Activating Protein (p135 SynGAP) Inhibited by CaM Kinase II." *Neuron* 20, no. 5 (May 1998): 895-904.

Chi, C. L. "The Isthmic Organizer Signal Fgf8 Is Required for Cell Survival in the Prospective Midbrain and Cerebellum." *Development* 130, no. 12 (Jun 2003): 2633-44.

Clement, J. P., M. Aceti, T. K. Creson, E. D. Ozkan, Y. Shi, N. J. Reish, A. G. Almonte*, et al.* "Pathogenic Syngap1 Mutations Impair Cognitive Development by Disrupting Maturation of Dendritic Spine Synapses." *Cell* 151, no. 4 (Nov 2012): 709-23.

Collins, A. L., D. Ma, P. L. Whitehead, E. R. Martin, H. H. Wright, R. K. Abramson, J. P. Hussman*, et al.* "Investigation of Autism and Gaba Receptor Subunit Genes in Multiple Ethnic Groups." *Neurogenetics* 7, no. 3 (Jul 2006): 167-74.

Dorey, K., and E. Amaya. "Fgf Signalling: Diverse Roles During Early Vertebrate Embryogenesis." *Development* 137, no. 22 (Nov 2010): 3731-42.

Dworkin, S., C. Darido, S. R. Georgy, T. Wilanowski, S. Srivastava, F. Ellett, L. Pase*, et al.* "Midbrain-Hindbrain Boundary Patterning and Morphogenesis Are Regulated by Diverse Grainy Head-Like 2-Dependent Pathways." *Development* 139, no. 3 (Feb 2012): 525-36.

Dworkin, S., and S. M. Jane. "Novel Mechanisms That Pattern and Shape the Midbrain-Hindbrain Boundary." *Cell Mol Life Sci* 70, no. 18 (Sep 2013): 3365-74.

Fatemi, S. H., T. J. Reutiman, T. D. Folsom, and P. D. Thuras. "Gaba(a) Receptor Downregulation in Brains of Subjects with Autism." *J Autism Dev Disord* 39, no. 2 (Feb 2009): 223-30.

Foley, J. E., M. L. Maeder, J. Pearlberg, J. K. Joung, R. T. Peterson, and J. R. Yeh. "Targeted Mutagenesis in Zebrafish Using Customized Zinc-Finger Nucleases." *Nat Protoc* 4, no. 12 (Dec 2009): 1855-67.

Force et al., 1999. "Preservation of Duplicate Genes by Complementary, Degenerative Mutations." *Genetics* 151, no.4 (Apr 1999): 1531-1545.

Fritschy, J. M. "Epilepsy, E/I Balance and Gaba(a) Receptor Plasticity." *Front Mol Neurosci* 1, no. 5 (Mar 2008): 5.

Gatto, C. L., and K. Broadie. "Genetic Controls Balancing Excitatory and Inhibitory Synaptogenesis in Neurodevelopmental Disorder Models." *Front Synaptic Neurosci* 2, no. 4 (Jun 2010): 4.

Gogolla, N., J. J. Leblanc, K. B. Quast, T. C. Sudhof, M. Fagiolini, and T. K. Hensch. "Common Circuit Defect of Excitatory-Inhibitory Balance in Mouse Models of Autism." *J Neurodev Disord* 1, no. 2 (Jun 2009): 172-81.

Goldman, S., C. Wang, M. W. Salgado, P. E. Greene, M. Kim, and I. Rapin. "Motor Stereotypies in Children with Autism and Other Developmental Disorders." *Dev Med Child Neurol* 51, no. 1 (Jan 2009): 30-8.

Gonzalez, M. I. "The Possible Role of Gabaa Receptors and Gephyrin in Epileptogenesis." *Front Cell Neurosci* 7, no. 113 (Jul 2013): 1-7.

Grunwald, D. J. "A Revolution Coming to a Classic Model Organism." *Nat Methods* 10, no. 4 (Apr 2013): 303, 05-6.

Hallmayer, J., S. Cleveland, A. Torres, J. Phillips, B. Cohen, T. Torigoe, J. Miller*, et al.* "Genetic Heritability and Shared Environmental Factors among Twin Pairs with Autism." *Arch Gen Psychiatry* 68, no. 11 (Nov 2011): 1095-102.

Hamdan Et Al. "Mutations in *SYNGAP1* in Autosomal Nonsyndromic Mental Retardation." *The New England Journal of Medicine* 360, no. 6 (Oct 2009): 599-605.

Hamdan, F. F., H. Daoud, A. Piton, J. Gauthier, S. Dobrzeniecka, M. O. Krebs, R. Joober*, et al.* "De Novo Syngap1 Mutations in Nonsyndromic Intellectual Disability and Autism." *Biol Psychiatry* 69, no. 9 (May 2011): 898-901.

Hamdan, F. F., J. Gauthier, Y. Araki, D. T. Lin, Y. Yoshizawa, K. Higashi, A. R. Park*, et al.* "Excess of De Novo Deleterious Mutations in Genes Associated with Glutamatergic Systems in Nonsyndromic Intellectual Disability." *Am J Hum Genet* 88, no. 3 (Mar 2011): 306-16.

Herbert, 2011." SHANK3, the Synapse, and Autism." *The New England Journal of Medicine* 365, no. 2 (Jul 2011): 173-175.

Hesselson, D., R. M. Anderson, M. Beinat, and D. Y. Stainier. "Distinct Populations of Quiescent and Proliferative Pancreatic Beta-Cells Identified by Hotcre Mediated Labeling." *Proc Natl Acad Sci U S A* 106, no. 35 (Sep 2009): 14896-901.

Higley, M. J., and D. Contreras. "Balanced Excitation and Inhibition Determine Spike Timing During Frequency Adaptation." *J Neurosci* 26, no. 2 (Jan 2006): 448-57.

Hwang, W. Y., Y. Fu, D. Reyon, M. L. Maeder, S. Q. Tsai, J. D. Sander, R. T. Peterson, J. R. Yeh, and J. K. Joung. "Efficient Genome Editing in Zebrafish Using a Crispr-Cas System." *Nat Biotechnol* 31, no. 3 (Mar 2013): 227-9.

Kaufman, L., M. Ayub, and J. B. Vincent. "The Genetic Basis of Non-Syndromic Intellectual Disability: A Review." *J Neurodev Disord* 2, no. 4 (Dec 2010): 182-209.

Kupfer et al. "Diagnostic and Statistical Manual of Mental Disorders". *Ame Psych Asso* 5, no. 10 (Jun 2013): 1176.

Kim Et Al." SynGAP: a Synaptic RasGAP that Associates with the PSD-95/SAP90 Protein Family." *Neuron* 20, no.4 (April 1998): 683-691.

Kim Et Al., 2003." The Role of Synaptic GTPase-Activating Protein in Neuronal Development and Synaptic Plasticity." *The Journal of Neuroscience* 23, no. 4 (Feb 2003): 1119-1124.

Kim Et Al., 2011." Prevalence of Autism Spectrum Disorders in a Total Population Sample." *Am J Psychiatry* 168, no.9 (Sep 2011): 904–912.

Klitten, L. L., R. S. Moller, M. Nikanorova, A. Silahtaroglu, H. Hjalgrim, and N. Tommerup. "A Balanced Translocation Disrupts Syngap1 in a Patient with Intellectual Disability, Speech Impairment, and Epilepsy with Myoclonic Absences (Ema)." *Epilepsia* 52, no. 12 (Dec 2011): e190-3.

Knuesel, I., A. Elliott, H. J. Chen, I. M. Mansuy, and M. B. Kennedy. "A Role for Syngap in Regulating Neuronal Apoptosis." *Eur J Neurosci* 21, no. 3 (Feb 2005): 611-21.

Kogan, M. D., S. J. Blumberg, L. A. Schieve, C. A. Boyle, J. M. Perrin, R. M. Ghandour, G. K. Singh*, et al.* "Prevalence of Parent-Reported Diagnosis of Autism Spectrum Disorder among Children in the Us, 2007." *Pediatrics* 124, no. 5 (Nov 2009): 1395-403.

Kohashi, T., and Y. Oda. "Initiation of Mauthner- or Non-Mauthner-Mediated Fast Escape Evoked by Different Modes of Sensory Input." *J Neurosci* 28, no. 42 (Oct 2008): 10641-53.

Krepischi, A. C., C. Rosenberg, S. S. Costa, J. A. Crolla, S. Huang, and A. M. Vianna-Morgante. "A Novel De Novo Microdeletion Spanning the Syngap1 Gene on the Short Arm of Chromosome 6 Associated with Mental Retardation." *Am J Med Genet A* 152A, no. 9 (Sep 2010): 2376-8.

Lambert, A. M., J. L. Bonkowsky, and M. A. Masino. "The Conserved Dopaminergic Diencephalospinal Tract Mediates Vertebrate Locomotor Development in Zebrafish Larvae." *J Neurosci* 32, no. 39 (Sep 2012): 13488-500.

Langheinrich, U. "Zebrafish: A New Model on the Pharmaceutical Catwalk." *Bioessays* 25, no. 9 (Sep 2003): 904-12.

Leonard, H., and X. Wen. "The Epidemiology of Mental Retardation: Challenges and Opportunities in the New Millennium." *Ment Retard Dev Disabil Res Rev* 8, no. 3 (Sep 2002): 117-34.

Liu et al. "Dlx Genes Encode DNA-Binding Proteins That Are Expressed in an Overlapping And Sequential Pattern During Basal Ganglia Differentiation." *Dev Dynam* 210, no. 4 (Dec 1997):498–512.

Lynch et al. " The Probability of Duplicate Gene Preservation by Subfunctionalization." *Genetics* 154, no. 1 (Jan 2000): 459-473.

Ma, D. Q., P. L. Whitehead, M. M. Menold, E. R. Martin, A. E. Ashley-Koch, H. Mei, M. D. Ritchie*, et al.* "Identification of Significant Association and Gene-Gene Interaction of Gaba Receptor Subunit Genes in Autism." *Am J Hum Genet* 77, no. 3 (Sep 2005): 377-88.

Marin Et Al., 2001." A Long, Remarkable Journey: Tangential Migration In The Telencephalon." *Nature* 2, no.11 (Nov 2001): 780-790.

Metin, C., J. P. Baudoin, S. Rakic, and J. G. Parnavelas. "Cell and Molecular Mechanisms Involved in the Migration of Cortical Interneurons." *Eur J Neurosci* 23, no. 4 (Feb 2006): 894-900.

Miller, J. A., S. L. Ding, S. M. Sunkin, K. A. Smith, L. Ng, A. Szafer, A. Ebbert*, et al.* "Transcriptional Landscape of the Prenatal Human Brain." *Nature* 508, no. 7495 (Apr 2014): 199-206.

Mione, M., D. Baldessari, G. Deflorian, G. Nappo, and C. Santoriello. "How Neuronal Migration Contributes to the Morphogenesis of the Cns: Insights from the Zebrafish." *Dev Neurosci* 30, no. 1-3 (Dec 2007): 65-81.

Mitchell, K. J. "The Genetics of Neurodevelopmental Disease." *Curr Opin Neurobiol* 21, no. 1 (Feb 2011): 197-203.

Mittmann, W., U. Koch, and M. Hausser. "Feed-Forward Inhibition Shapes the Spike Output of Cerebellar Purkinje Cells." *J Physiol* 563, no. 2 (Mar 2005): 369-78.

Myers et al. "Development and Axonal Outgrowth of Identified Motoneurons in the Zebrafish." *The journal of Neuroscience* 6, no. 8 (Aug 1996): 2278-2289.

Nalefski et al." The C2 Domain Calcium-binding Motif: Structural and functional diversity." *Protein Science* 5, no.12 (Dec 1996):2375-2390.

Normes et al. "Zebrafish Contains Two Pax6 Genes Involved In Eye Development." *Mechanisms of Development* 77*,* no.2 (Oct 1998): 185-196.

Panganiban et al. "Developmental Functions of the Distal-less/Dlx Homeobox Genes." *Development* 129, no. 19 (Oct 2002): 4371-4386.

Pena, V., M. Hothorn, A. Eberth, N. Kaschau, A. Parret, L. Gremer, F. Bonneau, M. R. Ahmadian, and K. Scheffzek. "The C2 Domain of Syngap Is Essential for Stimulation of the Rap Gtpase Reaction." *EMBO Rep* 9, no. 4 (Apr 2008): 350-5.

Petralia et al." Ontogeny of Postsynaptic Density Proteins at Glutamatergic Synapses." *Mol Cell Neurosci.* 29, no. 3 (July 2005): 436–452.

Pinto, D., A. T. Pagnamenta, L. Klei, R. Anney, D. Merico, R. Regan, J. Conroy*, et al.* "Functional Impact of Global Rare Copy Number Variation in Autism Spectrum Disorders." *Nature* 466, no. 7304 (Jul 2010): 368-72.

Porter, K., N. H. Komiyama, T. Vitalis, P. C. Kind, and S. G. Grant. "Differential Expression of Two Nmda Receptor Interacting Proteins, Psd-95 and Syngap During Mouse Development." *Eur J Neurosci* 21, no. 2 (Jan 2005): 351-62.

Raible, F., and M. Brand. "Divide Et Impera--the Midbrain-Hindbrain Boundary and Its Organizer." *Trends Neurosci* 27, no. 12 (Dec 2004): 727-34.

Rami. " Ischemic Neuronal Death in the Rat Hippocampus: the Calpain– calpastatin– caspase Hypothesis." *Neurobiology of Disease* 13, no.2 (Jul 2003): 75–88.

Repicky, S., and K. Broadie. "Metabotropic Glutamate Receptor-Mediated Use-Dependent Down-Regulation of Synaptic Excitability Involves the Fragile X Mental Retardation Protein." *J Neurophysiol* 101, no. 2 (Feb 2009): 672-87.

Rhinn Et Al." The Midbrain–hindbrain Boundary Organizer." *Current Opinion in Neurobiology* 11, no.1 (Feb 2001) :34–42.

Robu Et Al. "p53 Activation by Knockdown Technologies." *Plos Genetics* 3, no. 5 (May 2007): e78.

Ropers, H. H. "Genetics of Intellectual Disability." *Curr Opin Genet Dev* 18, no. 3 (Jun 2008): 241-50.

Santoriello, C., and L. I. Zon. "Hooked! Modeling Human Disease in Zebrafish." *J Clin Invest* 122, no. 7 (Jul 2012): 2337-43.

Sebat, J., B. Lakshmi, D. Malhotra, J. Troge, C. Lese-Martin, T. Walsh, B. Yamrom*, et al.* "Strong Association of De Novo Copy Number Mutations with Autism." *Science* 316, no. 5823 (Apr 2007): 445-9.

Sgado, P., L. Alberi, D. Gherbassi, S. L. Galasso, G. M. Ramakers, K. N. Alavian, M. P. Smidt, R. H. Dyck, and H. H. Simon. "Slow Progressive Degeneration of Nigral Dopaminergic Neurons in Postnatal Engrailed Mutant Mice." *Proc Natl Acad Sci USA* 103, no. 41 (Oct 2006): 15242-7.

Stoner, R., M. L. Chow, M. P. Boyle, S. M. Sunkin, P. R. Mouton, S. Roy, A. Wynshaw-Boris*, et al.* "Patches of Disorganization in the Neocortex of Children with Autism." *N Engl J Med* 370, no. 13 (Mar 2014): 1209-19.

Ting, J. T., J. Peca, and G. Feng. "Functional Consequences of Mutations in Postsynaptic Scaffolding Proteins and Relevance to Psychiatric Disorders." *Annu Rev Neurosci* 35 (Apr 2012): 49-71.

Verpelli, C., and C. Sala. "Molecular and Synaptic Defects in Intellectual Disability Syndromes." *Curr Opin Neurobiol* 22, no. 3 (Jun 2012): 530-6.

Voineagu, I et al. "Transcriptomic Analysis of Autistic Brain Reveals Convergent Molecular Pathology." *Nature* 474, no. 7351 (May 2011), 380-384.

Voineagu, I., and V. Eapen. "Converging Pathways in Autism Spectrum Disorders: Interplay between Synaptic Dysfunction and Immune Responses." *Front Hum Neurosci* 7, no. 738 (Nov 2013): 738.

Westerfield. A Guide for the Laboratory Use of Zebrafish Danio (Brachydanio) Rerio, 4th ed., Univ. of Oregon Press, Eugene (2000).

Wehr et al. "Balanced Inhibition Underlies Tuning and Sharpens Spike Timing in Auditory Cortex " *Nature* 426, no. 6965 (Nov 2003): 442-446.

Westin and Lardelli. "Three Novel Notch Genes in Zebrafish: Implications for Vertebrate Notch Gene Evolution and Function." *Dev. Genes Evol*. 207 no. 1 (May 1997): 51-63.

Wilent, W. B., and D. Contreras. "Dynamics of Excitation and Inhibition Underlying Stimulus Selectivity in Rat Somatosensory Cortex." *Nat Neurosci* 8, no. 10 (Oct 2005): 1364-70.

Yizhar, O., L. E. Fenno, M. Prigge, F. Schneider, T. J. Davidson, D. J. O'Shea, V. S. Sohal*, et al.* "Neocortical Excitation/Inhibition Balance in Information Processing and Social Dysfunction." *Nature* 477, no. 7363 (Sep 2011): 171-8.

Yu, M., Y. Xi, J. Pollack, M. Debiais-Thibaud, R. B. Macdonald, and M. Ekker. "Activity of Dlx5a/Dlx6a Regulatory Elements During Zebrafish Gabaergic Neuron Development." *Int J Dev Neurosci* 29, no. 7 (Nov 2011): 681-91.

Zollino, M., F. Gurrieri, D. Orteschi, G. Marangi, V. Leuzzi, and G. Neri. "Integrated Analysis of Clinical Signs and Literature Data for the Diagnosis and Therapy of a Previously Undescribed 6p21.3 Deletion Syndrome." *Eur J Hum Genet* 19, no. 2 (Feb 2011): 239-42.